

Observations of slip patterns on the surface of fatigued gold using the scanning tunnelling microscope

J. C. GROSSKREUTZ

Department of Physics, University of Missouri-Kansas City, Kansas City, MO 64110, USA

C. Q. BOWLES, A. A. WAHAB

Department of Mechanical and Aerospace Engineering, University of Missouri-Truman Campus, Independence, MO 64050, USA

Observations of fatigue-induced slip patterns on the surface of polycrystalline gold (+99.9%) using the scanning tunnelling microscope (STM) are presented. The samples were cycled in four-point bending between zero and 0.0025 strain for 250 and 2500 cycles. STM observations of the sample fatigued for 250 cycles revealed broad slip bands 0.38–0.69 μm wide containing narrow slip bands 0.015–0.123 μm wide and fine slip lines 0.006 μm wide. The depth of these features are 20–57 nm for broad slip bands, 3–7 nm for narrow slip bands, and approximately 2–4 nm for fine slip lines. The sample fatigued for 2500 cycles showed similar values for the width of the slip bands and slip lines except that their depth was increased by a factor of between 2 and 4 times for the narrow slip bands and the fine slip lines. Apparent persistent slip bands (PSBs) spaced 2.4 μm , 300–500 nm deep were also observed. These results demonstrate that STM is a significant new tool for observing and distinguishing various types of fatigue-induced surface slip patterns on suitably prepared samples. The vertical resolution obtained with STM is vastly superior to current SEM and TEM methods.

1. Introduction

Observation of fatigue-induced slip bands on the surface of metals by means of the optical microscope, the scanning electron microscope (SEM), and the transmission electron microscope (TEM), including the scanning transmission electron microscope (STEM), are well-developed techniques. However, operation of these instruments is based on the wave properties of either light or electrons and the use of apertures and lenses to magnify and focus the observed images. These properties, by their very nature, impose a lower limit on the resolving power that can be obtained. Current SEM and STEM instruments are capable of resolving surface profile features that have widths or spacings of 0.01 μm in the horizontal X - Y plane, and heights/depths of $\sim 0.01 \mu\text{m}$ in the vertical Z direction, depending on the sample and its preparation. However, there is considerable uncertainty in height measurements due to the two-dimensional nature of the images. Further uncertainty can arise when samples are tilted.

The scanning tunnelling microscope (STM), on the other hand, operates on an entirely different principle [1], namely the variations in electron tunnelling current between a very sharp, scanning tip and the surface being scanned. The steep, exponential dependence of

this current on the separation distance between tip and surface permits lower limit horizontal resolution of ~ 0.2 – 0.3 nm and vertical resolution ~ 0.01 – 0.1 nm , depending on instrument design and the sample being observed [2]. Application of the STM to problems in materials science and engineering is an active field [3], but its use for examining the surfaces of materials subjected to fatigue stresses is just beginning to emerge [4, 5]. We present observations of surface slip patterns on electropolished gold specimens which have been cycled in bending.

Our objectives are: (1) to demonstrate that STM is a valid tool for observing slip lines and bands in the very early stages of fatigue fracture, and (2) to correlate the STM images with those obtained utilizing SEM and TEM to image the same or closely similar surface areas. This second objective is important because of the significant qualitative differences in STM images of these surface features compared to SEM and TEM images of the same or similar surfaces. Moreover, the STM images obtained at magnifications up to 300 times greater than those currently available from SEM and TEM require careful analysis and extrapolation in order to eliminate surface contamination effects and idiosyncracies of the STM instrument itself. As we shall demonstrate, the greatly superior depth resolu-

tion of the STM, together with its unique imaging mechanism, present some interpretational problems for the first-time user.

2. Experimental procedure

A modified Nanoscope I scanning tunnelling microscope equipped with a wide-scan head (maximum scan range in X and Y direction is $8.4 \mu\text{m} \times 6.9 \mu\text{m}$; maximum scan range in the vertical Z direction is $\pm 1.4 \mu\text{m}$) was used. The scanning probe was made from 0.25 mm tungsten wire, and the tip selectively etched electrolytically in concentrated NaOH . The modified STM is equipped with a sample stage that permits rectilinear, translational motion of $\pm 3.8 \text{ mm}$ in the X and Y scan directions. The STM is mounted on a laboratory isolation table to reduce vibrational noise. All observations were made at atmospheric pressure; however, the sample stage and scanning head are enclosed by a cylindrical stainless steel cover that provides thermal stability and electromagnetic shielding.

STM images are displayed on an oscilloscope CRT, either as a line-scan (isometric) image or as a grey-scale image. To obtain a line-scan image, the feedback voltage that is applied to the Z -piezo for the purpose of maintaining constant tunnelling current is added to the CRT Y scanning voltage. Consequently, surface ridges and valleys are displayed on the screen in perspective. To obtain the grey-scale image, the feedback voltage signal is used to modulate the intensity of the CRT electron beam; high surface ridges are bright and deep valleys are dark. Elevations in between have

varying degrees of intensity. In either case, a quantitative measure of the depth or height of a slip line or band can be obtained from the image using a Z -piezo calibration together with the record of Z feedback voltage during the scans. The scanning piezo sensitivity was calibrated in the vertical Z -direction as 9.44 nm V^{-1} using a helium-neon laser interferometer. The horizontal X - Y piezo scan sensitivity was calibrated by imaging a blazed gold replica grating with 4968 grooves/mm (spacing = $0.2 \mu\text{m}$). The mean X - Y calibrations obtained were X : 28.2 nm V^{-1} , and Y : 23.1 nm V^{-1} . Fig. 1 displays a $0.6 \mu\text{m} \times 0.6 \mu\text{m}$ scan image of the grating.

To avoid surface oxide layer effects as much as possible, polycrystalline gold (+99.9%) was selected for these experiments. Previous work [6, 7] has shown that rather evenly spaced slip lines and bands are observed on and near the surface of fatigue-cycled gold, and that the presence or absence of atmospheric air during cycling makes very little difference in their appearance. Fig. 2 displays TEM micrographs of the surface and near-surface of polycrystalline gold (+99.9%) fatigue cycled in ambient air [6, 7].

For the experiments reported here, the polycrystalline gold was rolled into sheets 0.25 mm thick and cut into samples $12 \text{ mm} \times 12 \text{ mm}$ square. Samples were annealed at 650°C for 1 h in air which resulted in a grain size of $0.3 \mu\text{m}$. The samples were then electropolished in an acetic acid/chromium trioxide solution at room temperature and mounted individually with cyanoacrylate cement on the surface of a flat plastic bar. Bars were cycled in four-point bending for 250 or 2500 cycles between zero and 0.0025 strain amplitude as measured by strain gauges attached to the gold.

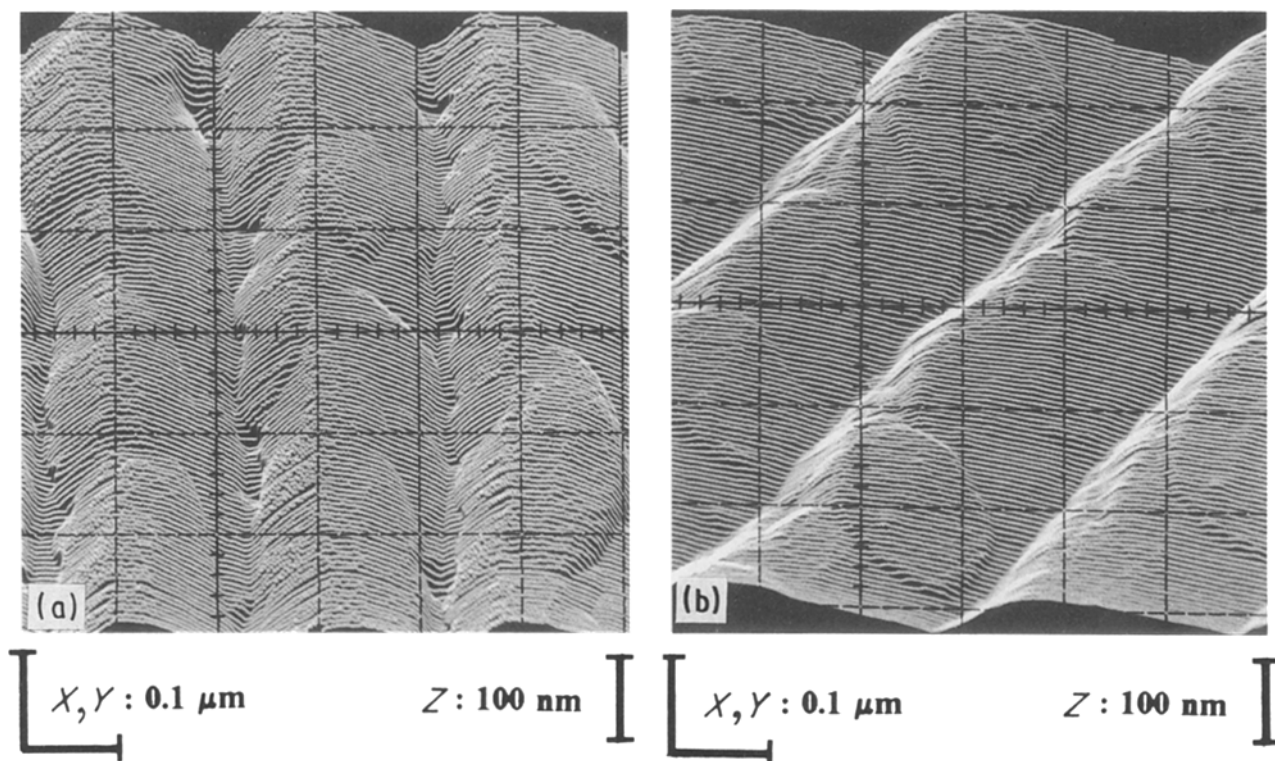


Figure 1 STM images of a blazed gold replica grating with 4968 grooves/mm; spacing between grooves = $0.2 \mu\text{m}$. Images were not electronically enhanced. (a) Grooves orientated at 90° to X -axis scan; X scan voltage setting = 21.3 V ; (b) grooves orientated at 45° to X -axis scan, X scan voltage setting = 21.3 V , Y scan voltage setting = 26.1 V .

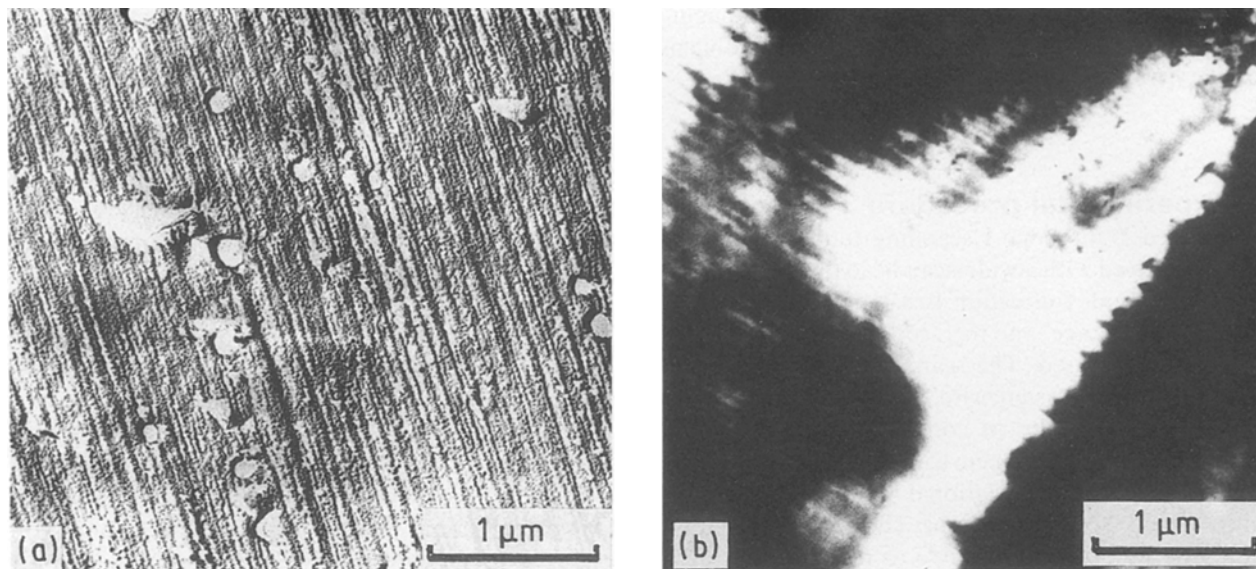


Figure 2 Transmission electron micrographs of slip bands formed at the surface of polycrystalline gold (99.9 + %) fatigued in ambient air for 10 000 cycles at ± 0.002 strain [6, 7]. (a) Surface replica (angle of shadow = 14°); (b) near-surface TEM of sample shown in (a) but not the same area, showing diffraction contrast at slip bands in upper left corner and grain boundary at lower right [5].

Examination of the surface of these samples by optical microscope ($\times 100$) revealed numerous grains containing slip bands.

Both uncycled and cycled sample surfaces were examined by STM and SEM. For the cycled sample surfaces, our procedure for identifying the area and the orientation of the slip lines on the gold grain to be observed by STM was as follows. (1) Identify a single grain containing slip by utilizing an optical microscope at $\times 40$ – 200 ; (2) draw a circle around the grain with a fine, felt-tip pen; and (3) note the direction/orientation of the slip bands by an arrow at the edge of the sample. The sample was then placed on the STM

stage, the slip oriented at 45° to the X and Y scan axes, and the STM scanning tip lowered to a position within the grain. Regular surface features on the STM image oriented at 45° to the scan axes could then be positively identified as slip bands and recorded. The STM images were obtained in the constant current mode with the tunnelling current maintained at 2.0 nA and the bias voltage maintained at 35 mV with the tip positive. For comparison with SEM observations, the same sample and similar procedures were used; however, we could not be certain that the exact same area of the grain was observed under both STM and SEM instruments.

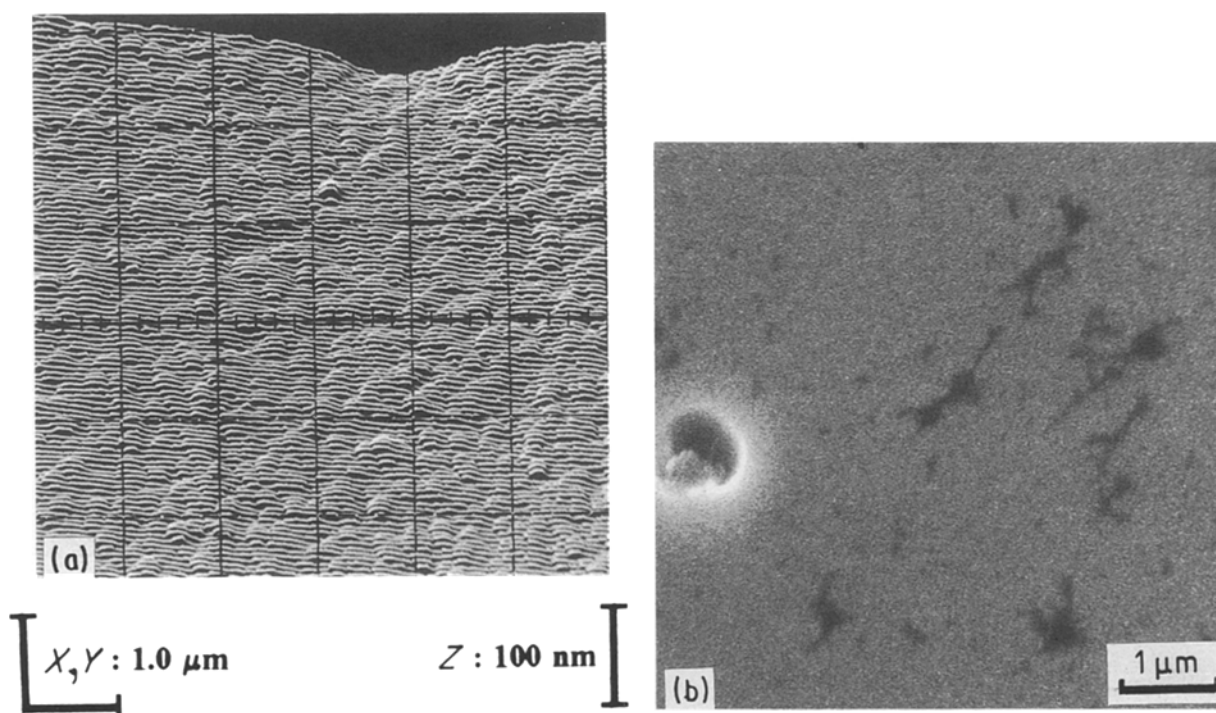


Figure 3 STM and SEM surface images of electropolished polycrystalline uncycled gold. STM image was not electronically enhanced. (a) $6 \mu\text{m} \times 6 \mu\text{m}$ STM scan, (b) $\times 13\,000$ SEM scan.

3. Results

3.1. Uncycled gold

The surface of uncycled, electropolished gold was examined with both STM and SEM in order to establish the “background” surface features. A typical, $6\ \mu\text{m} \times 6\ \mu\text{m}$ STM scan image is shown in Fig. 3a with the micrometre bar markers for the X - Y and Z dimensions. A rather random distribution of surface rills, most likely a product of the electropolishing, was observed. The average width of the rills is $0.22\ \mu\text{m}$, and the average depth is $3.4\ \text{nm}$. In order to obtain the surface detail shown, a high Z -gain setting on the

STM was required. Fig. 3b displays a typical SEM scan ($\times 13\ 000$) of the same sample and does not reveal any surface features other than random dust particles. This difference between STM and SEM images of the same electropolished surface illustrates the greatly superior depth resolution of the STM.

3.2. Fatigue-cycled gold

The surface of gold samples subjected to fatigue cycling were observed under both STM and SEM and compared. Fig. 4a (isometric line scan) and b (grey

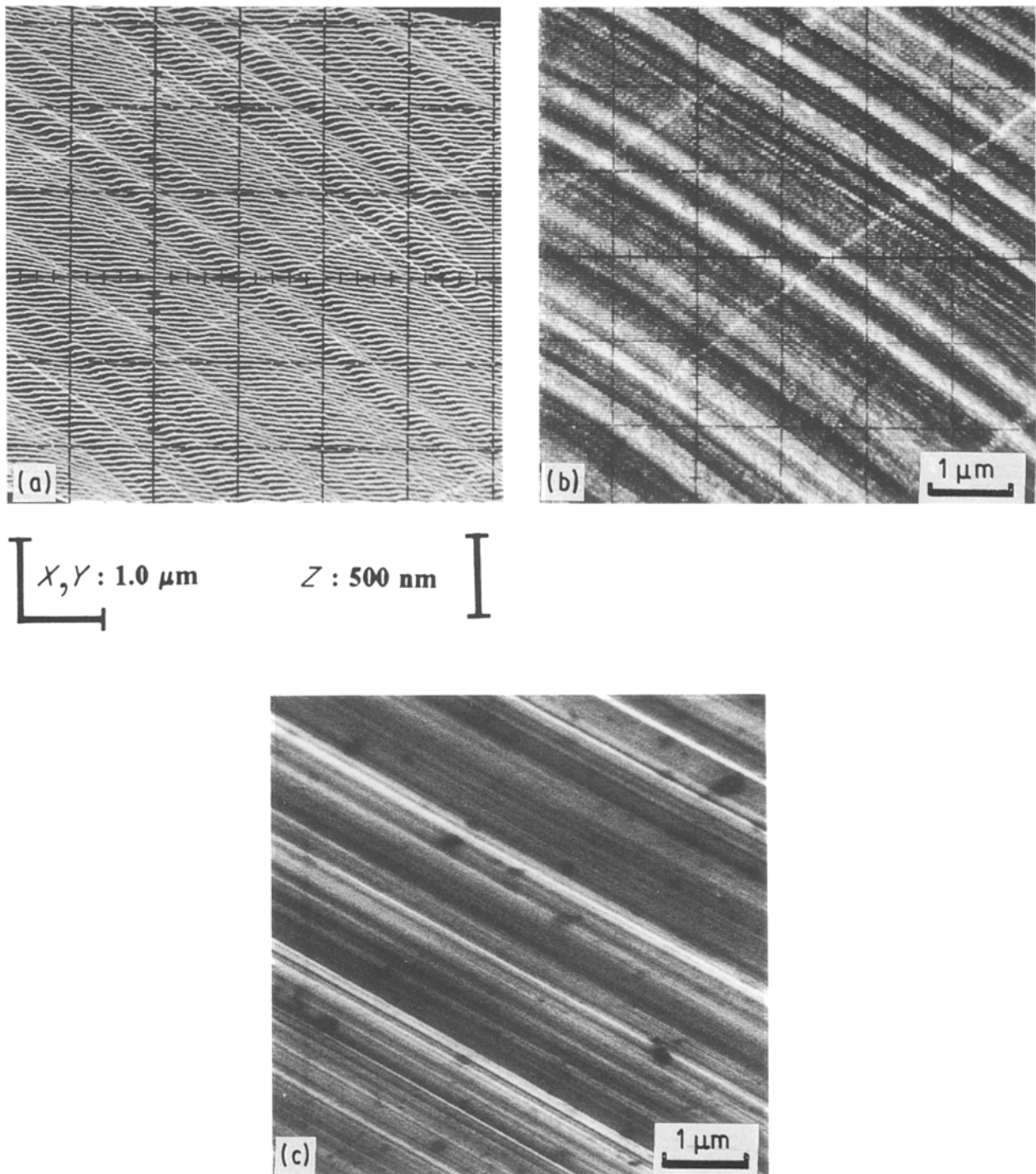


Figure 4 STM and SEM surface images of electropolished polycrystalline gold fatigued for 250 cycles at 0 – 0.0025 strain. STM images were not electronically enhanced. (a) $6\ \mu\text{m} \times 6\ \mu\text{m}$ isometric line scan STM image showing broad slip bands 0.38 – $0.69\ \mu\text{m}$ wide. (b) Grey scale STM image of the same area as in (a), (c) SEM image ($\times 13\ 000$) of nearby area; same grain as in (a) and (b). Clusters of slip bands corresponds to the slip bands in (a) and (b).

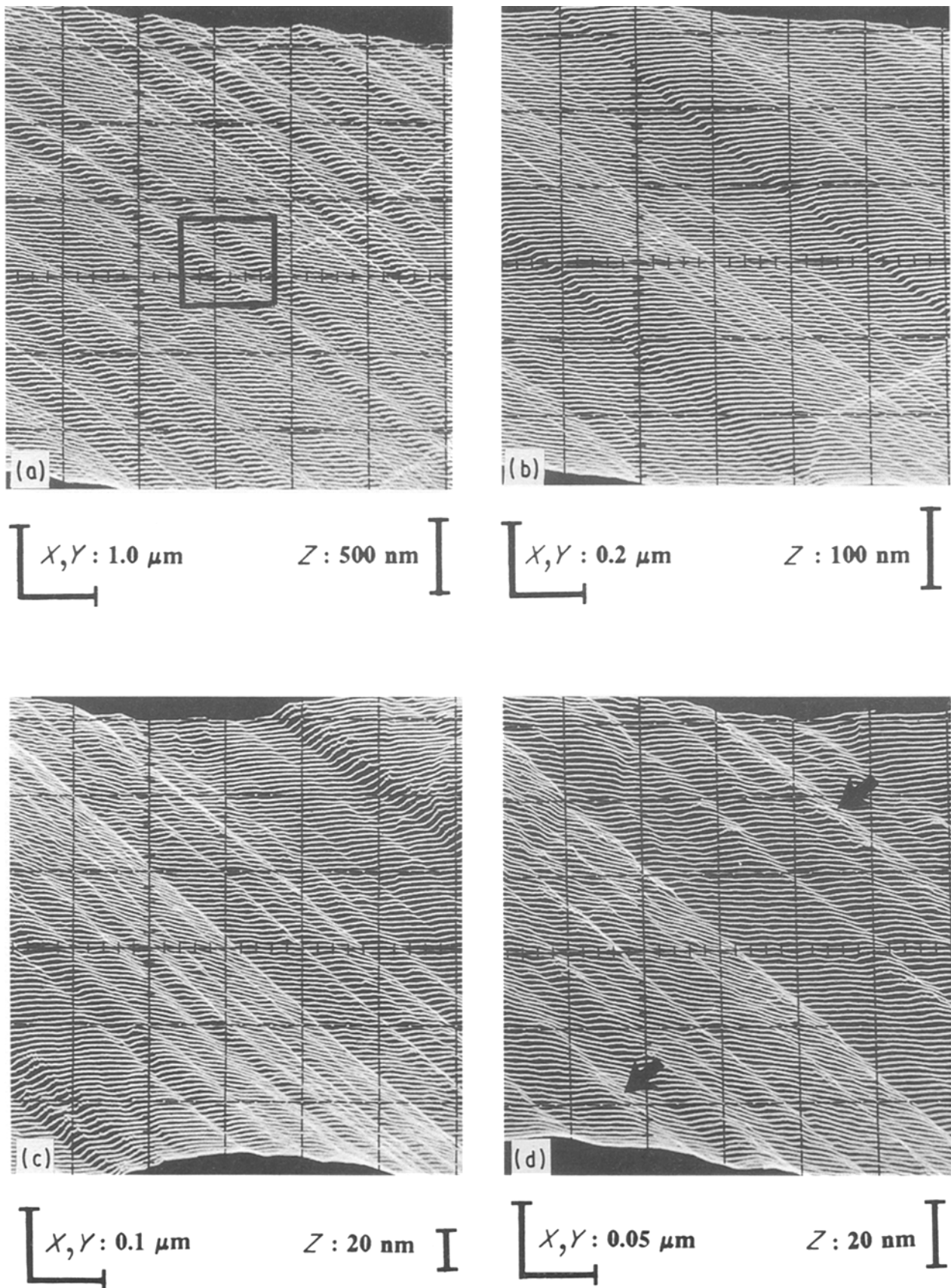
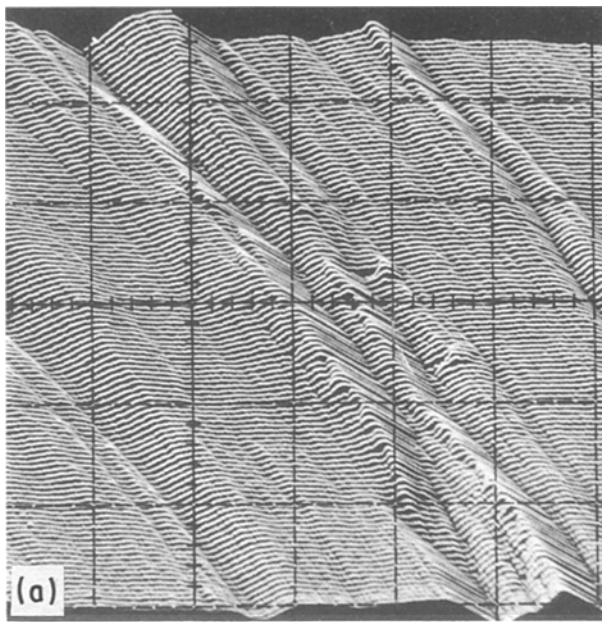


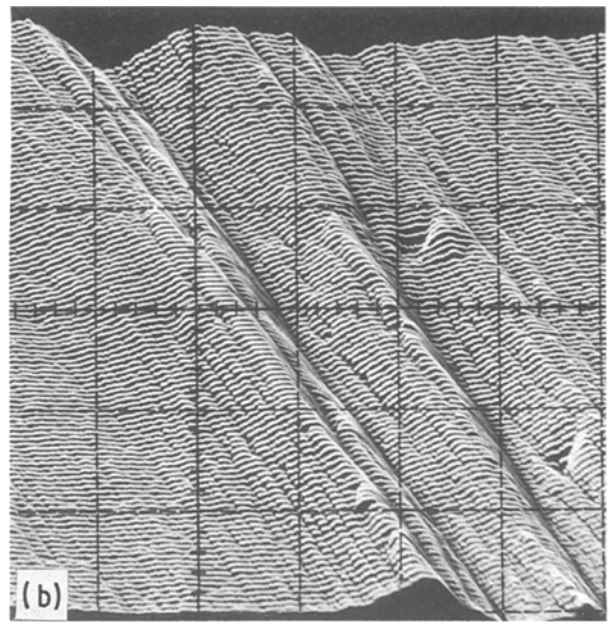
Figure 5 STM surface images of electropolished polycrystalline gold fatigued for 250 cycles at 0–0.0025 strain. The same area is shown at increasing magnification (smaller scan ranges) from (a)–(d). Images were not electronically enhanced. (a) $6 \mu\text{m} \times 6 \mu\text{m}$ scan showing broad slip bands $0.38\text{--}0.69 \mu\text{m}$ wide. Square box denotes area scanned in (b). (b) $1.2 \mu\text{m} \times 1.2 \mu\text{m}$ scan showing two broad slip bands $0.42 \mu\text{m}$ wide extending from the upper left corner to the lower right corner. (c) $0.6 \mu\text{m} \times 0.6 \mu\text{m}$ scan showing only one of the broad bands in (b), with numerous narrow slip bands clearly resolved on the slope of the broad band. (d) $0.3 \mu\text{m} \times 0.3 \mu\text{m}$ scan showing the narrow slip bands. Several narrow bands contain fine slip lines $0.006 \mu\text{m}$ wide (marked by arrows).

scale) display the same area of slip (produced by 250 cycles at 0–0.0025 strain amplitude) as imaged by a $6\ \mu\text{m} \times 6\ \mu\text{m}$ STM scan. The width of the broad slip bands varies from 0.38–0.69 μm across the images.

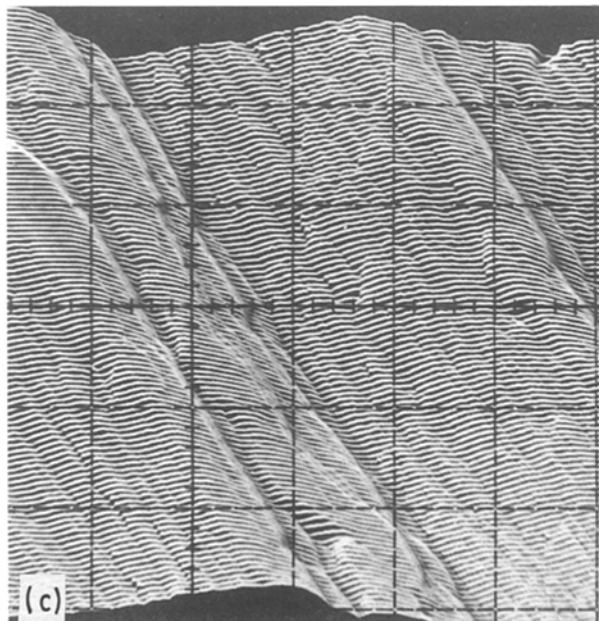
Their average depth/height is $\sim 43\ \text{nm}$. The grey scale image is bright along the top of slip bands and is dark along the valleys between the bands. Moreover, narrower slip bands are more easily seen in the grey scale



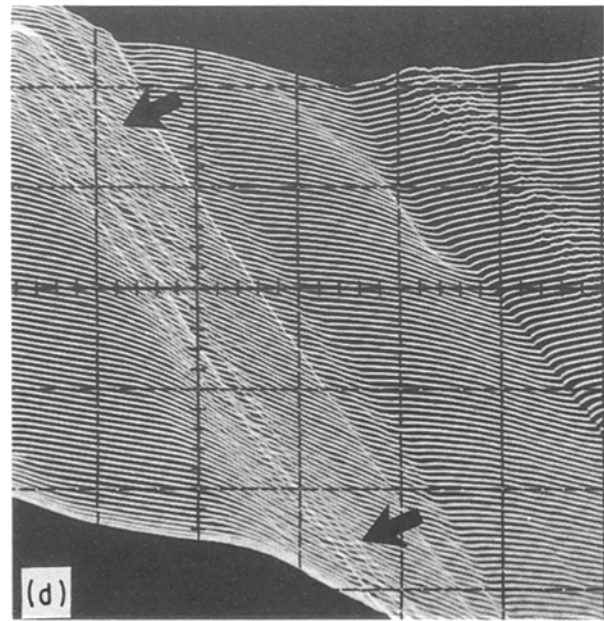
$X, Y: 1.0\ \mu\text{m}$ $Z: 1000\ \text{nm}$



$X, Y: 0.5\ \mu\text{m}$ $Z: 500\ \text{nm}$



$X, Y: 0.2\ \mu\text{m}$ $Z: 200\ \text{nm}$



$X, Y: 0.02\ \mu\text{m}$ $Z: 50\ \text{nm}$

Figure 6 STM surface images of electropolished polycrystalline gold fatigued for 2500 cycles at 0–0.0025 strain. Images were not electronically enhanced. (a) $6\ \mu\text{m} \times 6\ \mu\text{m}$ scan showing intense slip occurring approximately $2.4\ \mu\text{m}$ apart. (b) $3\ \mu\text{m} \times 3\ \mu\text{m}$ scan of the same area as in (a) reshewing more clearly narrow slip bands spaced 0.38–0.76 μm apart. (c) $1.2\ \mu\text{m} \times 1.2\ \mu\text{m}$ scan area of same area. (d) $0.12\ \mu\text{m} \times 0.12\ \mu\text{m}$ scan showing fine slip lines on a slope of a narrow band. Slip lines are spaced 1.5–3.8 nm apart and 2.3–4.7 nm deep (marked by arrows).

TABLE I Summary of slip band widths and heights^a

Method	Figure	Broad slip bands		Narrow slip bands		Fine slip bands	
		Width (μm)	Depth (nm)	Width (μm)	Depth (nm)	Width (μm)	Depth (nm)
TEM	2a			0.06			
	2b			0.04			
SEM	4c	0.46–0.70 (av. = 0.61)		0.03–0.07 (av. = 0.05)			
STM (250 cycles)	5a	0.38–0.69	38–57				
	5b	0.42	22	0.023–0.123	3.7–7.3		
	5c	0.47	20	0.023–0.115	2.8–7.0		
	5d			0.015–0.063	2.6	0.006	1.7
STM (2500 cycles)	6a	0.29–0.61 ^b	47–71				
	6b	0.27–0.50	32–47	0.038–0.113	15.8–31.5		
	6c			0.015–0.054	11.8–23.6		
	6d			0.038	9.4	0.002– 0.004	2.3– 4.7

^a Values are given as a range whenever there are more than one set of measurements taken. A single value of width or depth indicates only one measurement taken.

^b Average spacings between apparent PSBs = 2.4 μm .

image. On the other hand, three-dimensional perspective and quantitative measurement of the slip band height/depth is much easier to accomplish on the isometric line scan image. The comparable SEM image is displayed in Fig. 4c. The grey scale STM image (Fig. 4b) displays the same structure as the SEM image and appears to contain the same information. The similarities between the STM and SEM images in Fig. 4 are evident: on the SEM image, the broad bands of bright narrow lines, separated by dark breaks that occur at $\sim 0.5 \mu\text{m}$ intervals, correspond to the broad slip bands seen in Fig. 4a. The similarities between Fig. 4b and c are easier to discern because they are both grey scale intensity images of the same gold grain, but not exactly the same area as in the case for Fig. 4a and b.

Careful examination of Fig. 4a and b reveals a slight convex curvature of the slip bands when viewed at shallow angles along the direction of slip. This “pincushion” effect is an artefact of wide scan STM heads and is a result of a small non-linearity in the extremities of the *X* and *Y* axis piezo scan. The scanning tip describes arcs in the *XZ* and *YZ* planes that are centred at the top of the piezo. Hence when the image is projected to a flat surface, the extremities are slightly compressed. The effect is not noticeable at *X* and *Y* scan ranges less than about $2 \mu\text{m} \times 2 \mu\text{m}$.

A series of STM images taken at shorter and shorter scan ranges over the same area is shown in Fig. 5. For reference purposes, Fig. 5a–d are micrographs of the same region as marked by the square in Fig. 5a. Finer and finer slip detail can be seen. Note the two broad slip bands at the centre of (a), each $0.6 \mu\text{m}$ wide. These two bands fill most of (b) and run from the top left corner to the lower right corner. In (c), only one of these broad bands appears, the leftmost one in (b). Fig. 5d shows the downward slope of the broad band seen in Fig. 5c. The smallest slip resolved in this figure has a width of $0.006 \mu\text{m}$. The depth/height of these

slip features decreases from about 57 nm in (a) to 1.7 nm in (d).

Fig. 6a–d are STM images of a sample fatigued for 2500 cycles at a 0.0025 strain amplitude. Coarser and more well-defined slip bands are seen in Fig. 6a when compared to Fig. 5a as should be expected with the increased number of cycles. However, as the magnification is increased with smaller STM scan ranges (Fig. 6b–d) fine slip is still observed within the coarse slip bands. The smallest slip features observed in Fig. 6d are $0.002 \mu\text{m}$ wide and 2.3 nm high.

Table I is a summary of slip band widths and heights observed in our work. Data was obtained from both STM and SEM images. The categorization into broad slip bands, narrow slip bands, and fine slip lines is primarily for convenience. We do not address the physical significance of this “natural” division.

The images shown on Figs 5 and 6 illustrate the increasing resolution of surface slip patterns on fatigue-cycled gold as the STM scan range is decreased and the magnification thereby increased. This phenomenon of increased resolution with decreasing STM scan range does not occur when the SEM is used to image slip patterns. Companion photographs to Fig. 4c were taken (not shown) at $\times 56\,400$ and $\times 82\,600$ but no new features were observed, and images were increasingly less sharp. The SEM can be particularly susceptible to this problem when surface heights (*Z*-direction) are very small, which is the case for fine slip.

4. Discussion

4.1. Suitability and advantages of STM for observation of surface slip patterns

The observations presented in the previous section demonstrate that STM is a powerful tool for observing and distinguishing the various types of fatigue-

induced slip on the surface of high-purity gold. The interpretation of our results has been verified by comparison with SEM and TEM images of the same or similar gold surfaces where possible, and has been extrapolated to much higher STM magnifications by logical inference and by past experience with fatigued fcc metals.

The resolving power of the instrument in the nanometre region is clearly superior to the alternative SEM and TEM options, as shown by the quantitative results in Table I. These results demonstrate horizontal resolution of slip bands using the STM that is four to five times better than SEM or TEM. The vertical resolution is vastly superior, having the capability to detect early surface slip extrusions on gold of 6–8 Burgers vectors (1.7–2.3 nm) above the surface.

Our results reflect the usual development of sharply heterogeneous surface slip with increasing cycles of fatigue strain in pure fcc metals. Fig. 5a shows early development of broad slip bands, spaced on average 0.6 μm apart, that fill the surface after 250 cycles at 0–0.0025 strain. At higher magnifications, Fig. 5b and c display narrow slip bands ~ 0.02 – $0.12 \mu\text{m}$ wide that are superimposed on the broad bands. The height/depth of these slip features range from 3–7 nm for narrow slip bands and 20–57 nm for broad slip bands. These dimensions represent the passage of from 10–200 dislocations through the surface as the slip bands were formed. After 2500 cycles, plastic strain is localized into apparent persistent slip bands (PSBs) spaced on the average 2.4 μm apart, as shown in Fig. 6a. In between these persistent bands there are broad slip bands that are only marginally higher than at 250 cycles (Fig. 6a and b).

The PSBs in Fig. 6a are composed of two to three broad slip bands in which the plastic fatigue strains have been concentrated to produce surface contours that are now 300–500 nm deep, seven to eight times greater than those produced after only 250 strain cycles (Fig. 5a). A closer look at these deep valleys and ridges on Fig. 6b–d reveals the presence of narrow slip bands and fine slip lines, approximately the same width as those seen after 250 cycles, but which are now deeper by a factor of three to four times. The smallest fine slip lines we have observed are seen within these PSBs on Fig. 6d. They have widths of 0.002–0.004 μm and heights of 2.3–4.7 nm. These small dimensions correspond roughly to the emergence of approximately ten dislocations through the surface during the cyclic straining.

No other observational technique has, to our knowledge, produced this level of resolution for fatigue-induced slip processes. The slip patterns seen in Fig. 6 are very probably precursors of fatigue crack initiation in gold. In fact, Sriram *et al.* [4] have already demonstrated the STM capability to detect the initiation of very small fatigue cracks 0.1 μm in depth on the surface of pure silver. Our observations thus open the way to additional research on pre-crack initiation mechanisms at the surface of fatigue-cycled metals.

A further advantage of STM is that it can be operated under ambient air conditions, in vacuum, and in various controlled environments, including surfaces

covered with a liquid film, for the study of corrosion fatigue mechanisms.

4.2. Limitations of STM

Operation of the STM depends on establishing a very small tunnelling current between the scanning tip and the sample being imaged. Therefore, conducting or semiconducting surfaces are required for STM observation. Surfaces of non-conducting materials, such as most ceramics, or metals having oxide layers that are insulators (e.g. Al_2O_3) cannot be imaged faithfully. However, such surfaces may be covered with a thin, conducting film such as evaporated Pt–Pd or Pt–Ir, and a faithful image obtained. Such techniques have been utilized widely for imaging biological materials such as DNA with STM [8]. This problem may be sidestepped by using an atomic force microscope (AFM), which does not depend on the electronic properties of the surface being imaged, but is similar to the STM in resolution capabilities [9].

Surfaces having very rough profiles or rapid changes in slope can present problems if the STM feedback electronics controlling the vertical position of the scanning probe are not fast enough to raise the tip and prevent its “crashing” on to the surface. When this happens, the tip is usually blunted and is no longer able to function with high resolution. Replacement with a new tip is required, and locating the previous area of observation is usually difficult.

The STM lacks built-in “zoom” capability to observe a specific surface area over a large range of magnifications, i.e. several orders of magnitude. This capability would be very useful to follow and identify the mechanisms of surface crack nucleation and growth from onset of cycling to failure, especially in a controlled environment. Currently, only a combination of optical, SEM and STM instruments can achieve this goal.

4.3. Precautions in using STM

As with any new technique, there are some precautionary measures that should be understood when using STM to image surfaces. Some of the more important ones are listed below.

1. Interpretation of STM images requires experience and a good knowledge of STM operating and imaging mechanisms. The effects of image enhancement by the various electronic means available with most STMs should be thoroughly understood.

2. Surface contamination of the sample leads to artefacts on the images produced, and their accumulation in uncontrolled environments usually results in a gradual deterioration of the image during scanning.

3. The scanning tip should be resharpened or replaced periodically as observations proceed, in order to avoid the generation of artefacts in the surface image. It is very important to remember that the image is a convolution of the electronic structure of the surface and the tip.

4. Interpretation of images obtained from surfaces previously unexplored by STM may require verifying

experiments, e.g. such as comparison to SEM or TEM images of the same surface.

4.4. Other applications of STM for fatigue research

Observations of fatigue crack growth rates and mechanisms by means of STM is another attractive area of research [5]. As with slip band formation and crack initiation, the superior horizontal and depth resolution available allows observation of features hitherto unavailable for analysis. Such research will lead naturally to the development of STM as a tool for diagnostic fractography although surface roughness could present significant problems for observation of ductile materials.

5. Conclusions

On the basis of the present STM investigation of slip band patterns on the surface of partially fatigued polycrystalline gold, the following conclusions can be drawn.

1. STM is a suitable and powerful tool for observing and distinguishing the various types of fatigue-induced slip on the surface of high purity gold. This capability results from its vastly superior horizontal and vertical resolution compared to SEM and TEM. Interpretation of the STM images so obtained can be made and verified by comparison with SEM and TEM images of the same or similarly fatigued gold surfaces provided the difference in the imaging mechanisms of the STM and SEM/TEM are taken into account.

2. Slip band formation on the surface of pure gold fatigued cycled at 0–0.0025 strain in air begins within the first 250 cycles. Moreover, this slip can be characterized as broad slip bands (width = 0.38–0.69 μm) on which narrow slip bands (width = 0.015–0.123 μm) and fine slip lines (width = 0.006 μm) are superposed. The depth of these slip features range from 3–7 nm for narrow slip bands and 20–57 nm for broad slip bands.

3. Samples of pure gold fatigued at 0.0025 strain for 2500 cycles display localization of plastic strain in broad persistent slip bands that are spaced about 2.4 μm apart and with a depth of 300–500 nm, 7–8

times greater than after 250 strain cycles. These PSBs are very likely precursors of surface fatigue cracks on gold.

4. The height/depth of these slip bands and lines have been measured using STM with resolutions hitherto unobtained. Fine slip lines protruding above the gold surface by only 2–4 nm were observed. These dimensions corresponds to the emergence of roughly ten dislocations on the gold surface.

5. For observers familiar with imaging fatigued surfaces with SEM or TEM, interpretation of STM images requires experience and a good knowledge of STM operating and imaging mechanisms.

Acknowledgements

The authors thank Professor P. J. Bryant for use of the STM, Professor J. M. Phillips for fruitful discussions, and Mr R. G. Miller for his technical support. This research was partially supported by the University of Missouri-Kansas City through the Weldon Spring Endowment Fund.

References

1. Y. KUK and P. J. SILVERMAN, *Rev. Sci. Instrum.* **60** (1989) 165.
2. B. C. SCHARDT, S. YAU and F. RINALDI, *Science* **243** (1989) 1050.
3. M. P. EVERSON, R. C. JAKLEVIC and W. SHEN, *J. Vac. Sci. Technol. A* **8** (1990) 3662.
4. G. VENKATARAMAN, T. S. SRIRAM, M. E. FINE and Y. W. CHUNG, *Scripta Metall. Mater.* **24** (1990) 273.
5. J. LANKFORD and M. LONGMIRE, *J. Mater. Sci.* **26** (1991) 1131.
6. J. C. GROSSKREUTZ, *Acta Metall.* **13** (1965) 1269.
7. J. C. GROSSKREUTZ, and C. Q. BOWLES, in "Environment-Sensitive Mechanical Behavior of Materials", edited by A. R. C. Westwood and N. Stoloff (Gordon and Breach, New York, London, 1967) p. 67.
8. M. AMREIN, A. STASIAK, H. GROSS, E. STOLL and G. TRAVAGLINI, *Science* **240** (1988) 514.
9. S. A. C. GOULD, B. DRAKE, C. B. PRATER, A. L. WEISENHORN, S. MANNE, G. L. KELDERRMANN, H. J. BUTT, H. HANSMA, P. K. HANSMA, S. MAGANOV and H. J. CANTOW, *Ultramicroscopy* **33** (1990) 93.

Received 30 July

and accepted 28 November 1991